Available online at http://scik.org

J. Math. Comput. Sci. 11 (2021), No. 1, 793-808

https://doi.org/10.28919/jmcs/5208

ISSN: 1927-5307

EFFECT OF CHEMICAL REACTION ON MAGNETOHYDRODYNAMIC WILLIAMSON NANOFLUID WITH VARIABLE THICKNESS AND VARIABLE THERMAL CONDUCTIVITY

N. MANJULA[1,*], K. GOVARDHAN[2], M. N. RAJASHEKAR[3]

[1]Sreenidhi Institute of Science and Technology, Hyderabad, India

[2]Department of Mathematics, GITAM University, Hyderabad, India

[3]Department of Mathematics, JNTUH College of Engineering, Jagtial, India

Abstract: The effect of chemical reaction on an MHD boundary layer flow with variable thickness and variable thermal conductivity on a stretching sheet has been examined. Here is an investigation done on the chemical reaction parameter along with the slip parameter and velocity index parameter to a non-flat sheet. Similarity transformations are applied to convert the PDEs into a system of non-linear ODEs. The nonlinear coupled ODEs are boundary value problems. These are reduced to IVP by the shooting technique. Finally, the IVPs are solved by using the Adam-Bashforth Moulton method. The velocity, concentration, temperature profiles have been discussed for different parameters.

Keywords: MHD; Williamson nanofluid; chemical reaction parameter; viscous dissipation; stretching sheet.

2010 AMS Subject Classification: 76D05.

1. INTRODUCTION

Nanotechnology has been quickly growing in the recent years. The liquid containing nanometer-sized particles are called nanofluids. Nanoparticles range is between 1 and 100nm.

*Corresponding author

E-mail address: nagula_manju@yahoo.com

Received November 15, 2020

These nanoparticles comprise metals. For example-oxides, carbides and carbon nanotubes. Many industries require an energy-efficient heat transfer fluid. S.U.S. Choi & J.East man [1] introduced the fundamental vision of consolidating the nanoparticles inside the base fluid to upgrade the thermal conductivity. Buongiorno [2] built up a model with analytic solution for convective heat transfer in a Brownian diffusion of nanofluid. He watched the impact of diffusion and thermophoresis in nanofluid. Daungthongsuk and Wongwises [3], Wang [4], Mujumdar [5] and Kakac and Pramuanjaroenkij [6] have presented excellent results on the flow of nanofluids. A.V.Kuznetsov [7] studied the convective nanofluid in a vertical plate, later they extended their work for a permeable medium. The model is utilized for the nanofluid joins the impacts of Brownian motion and thermophoresis. N. Bachok, A. Ishak [8] described a nanofluid on a moving semi-infinite plate in a uniform stream to the steady boundary layer. In this plate, it is accepted to be moved in the equivalent or backwards path to the free stream. W. A. Khan, I. Pop [9] both investigated numerically the boundary layer laminar fluid stream from the extending of a level surface in nanofluid. In this nanofluid, it contains the effects of Brownian motion and thermophoresis. P. Rana and R. Bhargava [10] have studied laminar boundary layer steady state flow of a nanofluid over a nonlinearly extending sheet. In this additionally nanofluid, it consolidates the impacts of thermophoresis and Brownian motion. G. K. Ramesh et. al. [11] have explored the magneto hydrodynamic stagnation point flow on a non-level plate.It is stretched in this plate.And the effects of magnetic field and thermal radiation have also been investigated. In this paper, it has been observed that temperature and nanoparticles fraction distribution has increased due to the raising value of wall thickness parameter. Mahapatra & Gupta [12] have analyzed heat transfer in the stagnation point flow induced by a stretching sheet. The transient MHD laminar free convection stream of nanofluid has been examined by S. Mahmud et. al. [13]. The flow is past on a vertical surface which is permeable and extendable under increasing velocity. In this process, it has taken nanoparticles which are Al_2O_3 and Cu. Consequently, it has come to the modulus of skin friction coefficient.

M.M. Rashidi et. al. [14] have studied the boundary layer flow of nanofluids over a continuously moving surface. They researched the velocity and temperature profiles. R.V. Williamson [15] described the flow of pseudo plastic materials. S. Nadeem, S.T.Hussain [16] inspected the 2D flow of the Williamson fluid over an extending sheet under the impacts of nano-sized particle additionally depicted the nano Williamson fluid. Shagaiya et. al. [17] introduced nano fluid flow on non-linear extended surface with variable thickness in the occurrence of electric field.

In the present article, the numerical outcomes of Shazwani Md. Razi et. al. [18] have been replicated with a convincing agreement and extended by considering the chemical reaction.

2. MATHEMATICAL FORMULATION

Consider a 2D, laminar, incompressible MHD Williamson nanofluid flow through a plate in a porous medium. The starting point is here situated at cleavage from which the sheet is drawn through the fluid medium. The sheet has been stretched exponentially with velocity $U_x = U_0 (x+b)^m$, m is an index of velocity power, U_0 and b are dimensional constants. The sheet is moving along $x-$axis direction and it is a non-flat. The thickness of a sheet varies as $y = A(x+b)^{\frac{1-m}{2}}$. Here, A is a very small quantity so that the sheet is sufficiently thin. Magnetic field is applied to the perpendicular direction of fluid flow.

The governing equations for the above mathematical model is as follows.

$$\frac{\partial \bar{u}}{\partial x} + \frac{\partial \bar{v}}{\partial y} = 0 \tag{2.1}$$

$$\bar{u}\frac{\partial \bar{u}}{\partial x} + \bar{v}\frac{\partial u}{\partial y} = \upsilon \frac{\partial^2 \bar{u}}{\partial y^2} + \sqrt{2}\upsilon\Gamma \frac{\partial \bar{u}}{\partial y}\frac{\partial^2 \bar{u}}{\partial y^2} - \frac{\sigma B^2}{\rho}\bar{u} - \frac{\upsilon}{k}\bar{u} \tag{2.2}$$

$$\bar{u}\frac{\partial T}{\partial x} + \bar{v}\frac{\partial T}{\partial y} = \frac{1}{(\rho c_p)_f}\frac{\partial}{\partial y}\left(\kappa \frac{\partial T}{\partial y}\right) - \frac{1}{(\rho c_p)_f}\frac{\partial q_r}{\partial y} + \frac{(\rho c_p)_p}{(\rho c_p)_f}\left[D_B \frac{\partial C}{\partial y}\frac{\partial T}{\partial y} + \frac{D_T}{T_\infty}\left(\frac{\partial T}{\partial y}\right)^2\right] \tag{2.3}$$

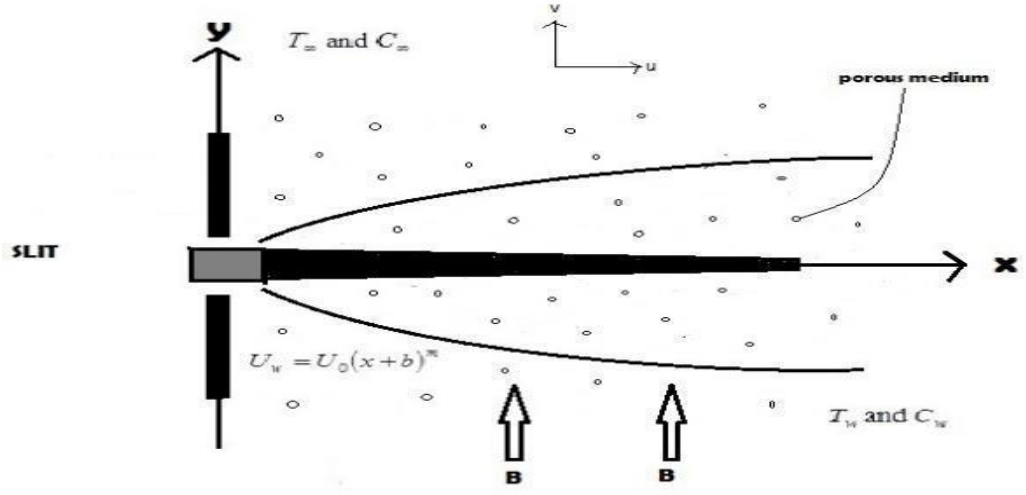

Figure 1. The coordinate system and fluid flowing.

$$\bar{u}\frac{\partial C}{\partial x}+\bar{v}\frac{\partial C}{\partial y}=D_B\frac{\partial^2 C}{\partial y^2}+\frac{D_T}{T_\infty}\frac{\partial^2 T}{\partial y^2}-k_0\left(C-C_\infty\right) \tag{2.4}$$

Where ρ is fluid density, Γ is material parameter, σ is electrical conductivity, k is porous medium permeability, $\tau=\frac{(\rho c)_p}{(\rho c)_f}$ where $(\rho c)_p$ is heat capacity of the nanoparticle material and $(\rho c)_f$ is heat capacity of fluid, $\kappa=\kappa_\infty\left(1+\omega\left(T-T_\infty\right)/\left(T_w-T_\infty\right)\right)$ is temperature dependent thermal conductivity where $\omega=\left(pc_p\right)_p/\left(pc_p\right)_f$, Tw is wall temperature of fluid, T_∞ is temperature ambient, D_B is Brownian diffusion Coefficient, D_T Coefficient of thermophoresis diffusion $B=B_0\left(x+b\right)^{\frac{m-1}{2}}$ is Magnetic field, $q_r=-\frac{4\sigma^*}{3k^*}\frac{\partial T^4}{\partial y}$ is Roseland approximation for radiation, σ^* is Stefan-Boltzmann constant and k^* mean absorption coefficient.

Boundary conditions can be written as

$$\left.\begin{aligned}&\bar{u}=U_w(x)+l_1\frac{\partial\bar{u}}{\partial y}=U_0(x+b)^m+l_1\frac{\partial\bar{u}}{\partial y},\bar{v}=0,T=T_w+l_2\frac{\partial T}{\partial y},\\&C=C_w+l_3\frac{\partial C}{\partial y}\qquad when\quad y=A(x+b)^{\frac{1-m}{2}}\\&\bar{u}=0,T=T_\infty,C=C_\infty\quad when\quad y\to\infty\end{aligned}\right\} \tag{2.5}$$

In Roseland approximation, Expand T^4 as a Taylor's series expansion and neglect the higher differentials then

$$\frac{\partial q_r}{\partial y}=-\frac{16\sigma^*{T_\infty}^3}{3k^*}\frac{\partial^2 T}{\partial y^2}.$$

The following process was implemented to convert the PDEs to ODEs

$$\left.\begin{aligned}
&\eta = \sqrt{\frac{U_0(m+1)}{2\upsilon}}\left[y(x+b)^{\frac{m-1}{2}} - A \right], \\
&\psi = \sqrt{\frac{2\upsilon U_0}{m+1}}(x+b)^{\frac{m-1}{2}}, \\
&\theta(\eta) = \frac{T - T_\infty}{T_w - T_\infty}, \\
&\phi(\eta) = \frac{C - C_\infty}{C_w - C_\infty}.
\end{aligned}\right\} \tag{2.6}$$

The final dimensionless form of the governing model is

$$f''' + ff'' + \lambda f'' f''' - \frac{2m}{m+1} f'^2 - (M + kp) f' = 0 , \tag{2.7}$$

$$\left(1 + \frac{4}{3}R + \varepsilon\theta\right)\theta'' + \varepsilon\theta'^2 + \Pr f\theta' + \frac{N_c}{L_e}\phi'\theta' + \frac{N_c}{L_e N_{bt}}\theta'^2 = 0 , \tag{2.8}$$

$$\phi'' + Le \Pr f\phi' + \frac{1}{N_{bt}}\theta'^2 - 2Sck_0(C_w - C_\infty)\phi = 0 \tag{2.9}$$

where

$$\lambda = \frac{\Gamma(m+1)^{\frac{1}{2}}(b+x)^{\frac{3m-1}{2}} U_0^{\frac{3}{2}}}{\upsilon^{\frac{1}{2}}}, M = \frac{2\sigma B_0^{\,2}}{(m+1)U_0\rho}(b+x)^{1-m}, k_p = \frac{2\upsilon(b+x)^{1-m}}{k(m+1)U_0},$$

$$R = \frac{4\sigma^* T_\infty^{\,3}}{k_\infty k^*}, \Pr = \frac{\upsilon}{\alpha}, L_e = \frac{\alpha}{D_B}, N_c = \frac{(\rho c)_p (C_w - C_\infty)}{(\rho c)_f}, \qquad N_{bt} = \frac{D_B T_\infty (C_w - C_\infty)}{DT(T_w - T_\infty)}.$$

The boundary condition (2.5) getting into the following dimensionless form

$$\left.\begin{aligned}
&f' = (n_1) f'' + 1 \quad f = \alpha\left(\frac{1-m}{m+1}\right) f', \quad \theta = (n_3)\theta + 1 \quad \phi(0) = (n_2)\phi + 1 \quad as \ \ \eta \to 0 \\
&f' \to 0, \theta \ \to 0 \ , \varphi \to 0 \quad as \ \ \eta \to \infty
\end{aligned}\right\} \tag{2.10}$$

$\alpha = A\sqrt{\frac{U_0(m+1)}{2\upsilon}} \rightarrow$ wall thickness parameter, $n_1 = l_1\sqrt{\frac{U_0(m+1)}{2\upsilon}}(x+b)^{\frac{m-1}{2}} \rightarrow$ velocity slip parameter, $n_2 = l_2\sqrt{\frac{U_0(m+1)}{2\upsilon}}(x+b)^{\frac{m-1}{2}} \rightarrow$ temperature slip parameter,

$n_3 = l_3\sqrt{\frac{U_0(m+1)}{2\upsilon}}(x+b)^{\frac{m-1}{2}} \rightarrow$nanoparticle volume fraction slip parameter.

3. SOLUTION METHODOLOGY

The equations (2.7), (2.8), (2.9) are coupled nonlinear boundary value ordinary differential equations. Their numerical solution has been obtained by converting into the first order initial value ODEs using shooting method. In this, it shoots our trajectories until it is discovered a trajectory that has the desired boundary value. In this process, the equations (2.7), (2.8) and (2.9) are rewritten and stated below.

$$f''' = \frac{-1}{1+\lambda f''}\left[-ff''+\frac{2m}{m+1}f'^{2}+(M+k_p)f'\right] \tag{3.1}$$

$$\theta'' = \frac{-1}{(1+\in\theta+\frac{4}{3}R)}\left[\Pr f\theta'+\frac{N_c}{L_e}\theta'\phi'+\frac{N_c}{N_{bt}L_e}\theta'^{2}\right] \tag{3.2}$$

$$\varphi'' = -L_e \Pr\ f\phi'-\frac{1}{N_{bt}}\theta''+2Sck_0(C_w-C_\infty)\phi \tag{3.3}$$

If it is used the following notations

$$f = y_1,\ \theta = y_4,\quad \phi = y_6$$

Further, it denotes

$$f'\ by\ y_2,\ f''\ by\ y_3,\ \theta'\ by\ y_5,\quad \phi'\ by\ y_7$$

Then, the equations (3.1), (3.2), (3.3) are reducing into the first order ODEs

$$y_1' = y_2, \qquad y_1(0) = \alpha\left(\frac{m+1}{1-m}\right)(1+n_1 r) \tag{3.4}$$

$$y_2' = y_3, \qquad y_2(0) = 1+n_1 r \tag{3.5}$$

$$y_3' = -\frac{1}{1+\lambda y_3}\left[-y_1y_3+\frac{2m}{m+1}y_2^2+\left(M+k_p\right)y_2\right],\quad y_3(0)=r, \tag{3.6}$$

$$y_4' = y_5, \qquad y_4(0) = 1+n_2\ s \tag{3.7}$$

$$y_5' = -\frac{1}{\left(1+\varepsilon y_4+\frac{4}{3}R\right)}\left[P_r y_1y_5+\frac{N_c}{L_e}y_5y_7+\frac{N_c}{N_{bt}L_e}y_5^2\right],\qquad y_5(0)=s \tag{3.8}$$

$$y_6' = y_7, \qquad y_6(0) = 1+n_3\ t \tag{3.9}$$

$$y_7' = -L_eP_r y_1y_7-\frac{1}{N_{bt}}y_5'+2S_ck_0\left(c_w-c_\infty\right)y_6, \qquad y_7(0)=t \tag{3.10}$$

For solving above system numerically, we replace the domain $(0,\eta_\infty)$ by the bounded domain $[0,M_\infty]$ where M_∞ is some suitable real number. In the above system of equations, we have $y_3(\eta), y_5(\eta), y_7(\eta)$ *at* $\eta = 0$ i.e. r, s, t are missing conditions and can be calculated by Newtoon-Raphson method until the following conditions are met.

$$\max(|y_2(\eta_\infty) - 0|, |y_4(\eta_\infty) - 0|, |y_6(\eta_\infty) - 0|) < 10^{-3}$$

4. NUMERICAL SOLUTIONS

In the present paper, the profiles of velocity, temperature and concentration have been analyzed. These profiles are expressed in terms of graphs for different choice of flow parameters. Effect of kp, R, Le, γ, Pr, λ on velocity, temperature and nanoparticle volume fraction profiles are discussed.

Table 1 depicts the comparison of skin friction coefficient, $f''(0)$ results obtained by Khader and Megahed [18], Reddy et.al. [19], Razi et. al. [20] and present outcomes are in good agreement.

Table 1. The correlation results for the skin friction coefficient, $f''(0)$ for m when

$$M = 0, \lambda = 0, kp = 0 \text{ and } \alpha = 0.5.$$

m	[18]	Reddy et. al. [19]	Razi et. al. [20]	Present results
0	0.9577	0.957644	0.957644	0.957661300
0.5	0.9798	0.979949	0.979949	0.979990700
1.0	1.0000	1.000008	1.000008	1.000062000
2.0	1.0234	1.023420	1.023420	1.023484000
3.0	1.0358	1.035883	1.035883	1.035950000
5.0	1.0486	1.048628	1.048628	1.048694000
7.0	1.0551	1.055062	1.055062	1.055127000
9.0	1.0588	1.058934	1.058934	1.058998000
10.0	1.0603	1.060343	1.060343	1.060406000

Fig 2 depicts the profile of velocity; Fig 3 shows the profile of temperature for three different values of velocity slip parameter n_1. In the present paper, decreasing of velocity profile to the raising of n_1 can be watched, just as fluid velocity inside the boundary layer because of the positive estimation of fluid velocity contiguous the outside of the sheet, so, it decreases the thickness of momentum boundary layer. Additionally, there is an expansion of fluid flow in the boundary layer to an increasing of n_1 which permits more fluid to fall past the sheet. Fig. 3 shows the increasing of temperature profile for an increasing of n_1 which prompts to the reducing of density of thermal boundary layer.

Fig 4 shows the decreasing the profile of temperature as an increasing of n_2 value. The temperature slip parameter n_2 decreases the $\theta(\eta)$ consequently the thickness of the temperature boundary layer reduces as the heat transfer from the surface to the fluid decreases.

Fig 5 shows the decreasing the profile of nanoparticle volume fraction for rising of nanoparticle volume fraction parameter n_3. Since slip parameter, n_3 interrupts the nanoparticle volume fraction in the fluid. Consequently, it goes to the decreasing of mass transfer from the surface to the fluid, so, the thickness of the layer has reduced.

Fig 6 shows the slight increasing of velocity profile to the rising of velocity power index m Figs. 7 and 8 show the increasing of heat and mass transfer as the plate is extended exponentially. So, the thickness of thermal and nanoparticle boundary layer have been increased.

Figs 9, 10, 11 show the decreasing of velocity, temperature and nanoparticle volume fraction profiles changing the wall thickness parameter like α=0, 0.6, 1.2 when $m<1$. And, it leads to the decrease on the boundary layers close to the plate respectively. But, the opposite behavior can be seen for $m>1$ in figures 12-14, i.e., the velocity, thermal, nanoparticle volume fraction profiles have increased as increasing values of α, because the movement of fluid flow is slow.

Fig 15 shows impact of γ on $\phi(\eta)$. By increasing γ, the nanoparticle volume fraction profile has been decreased.

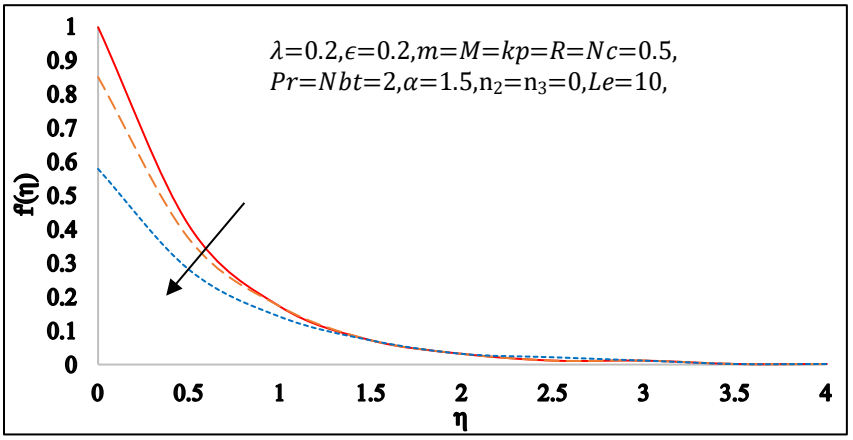

Figure 2. Impact of n_1 on f'

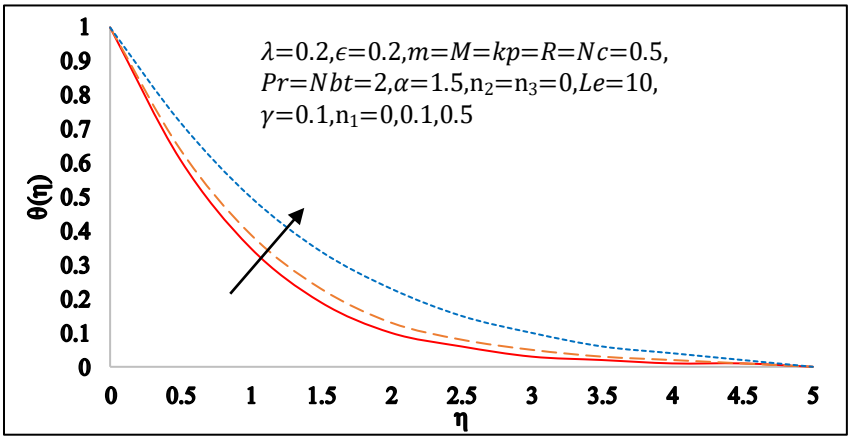

Figure 3. Impact of n_1 on θ

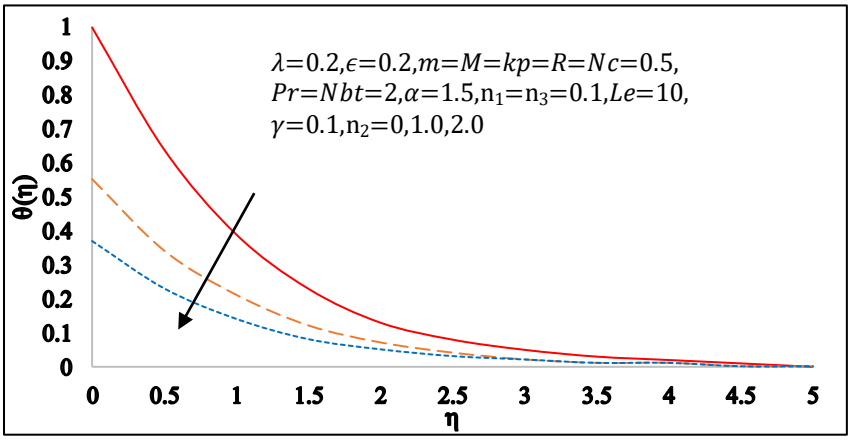

Figure 4. Impact of n_2 on θ

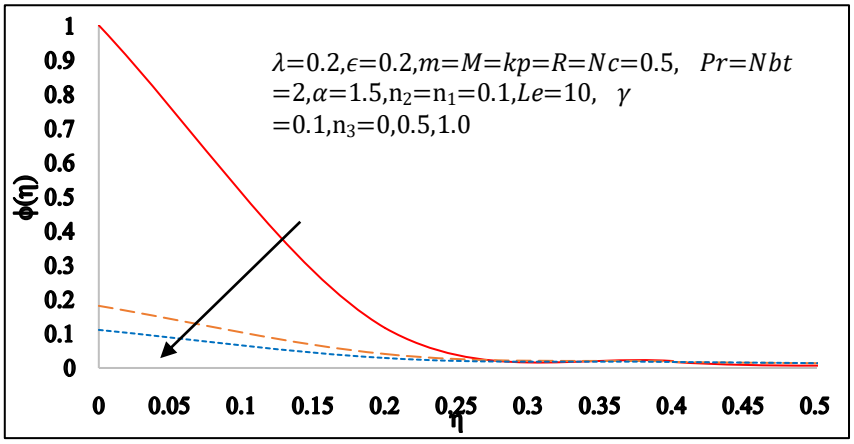

Figure 5. Impact of n_3 on ϕ

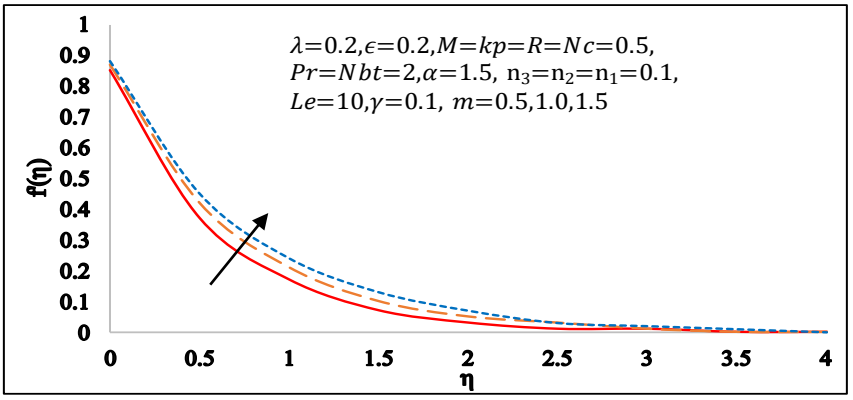

Figure 6. Impact of m on $f^{'}$

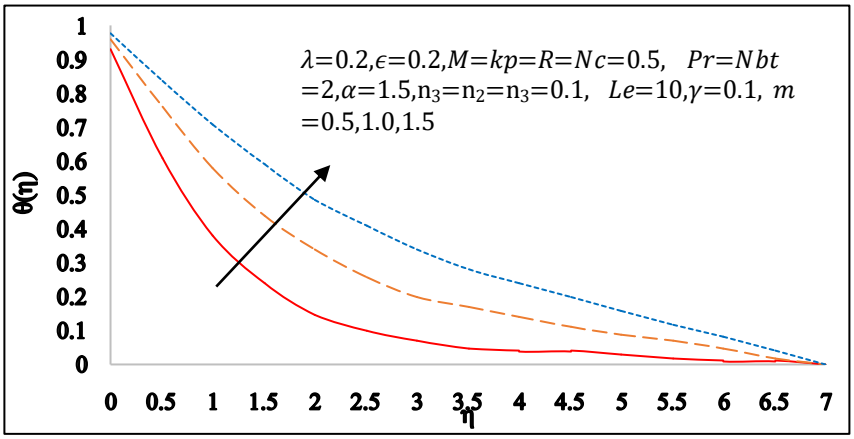

Figure 7. Impact of m on θ

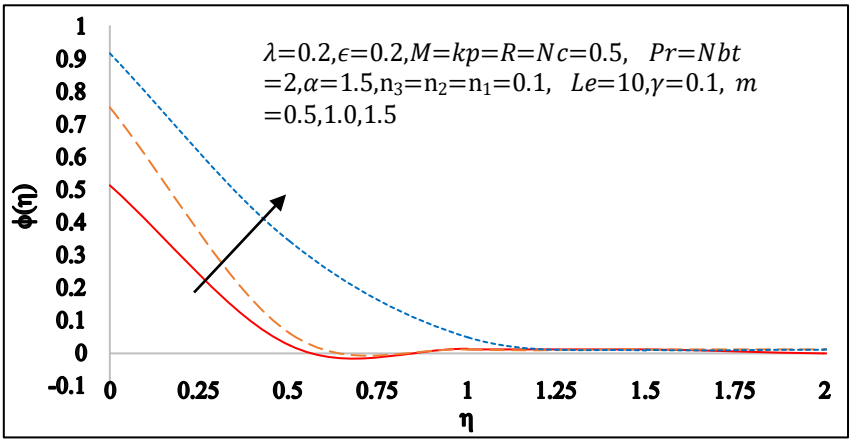

Figure 8. Impact of m on ϕ

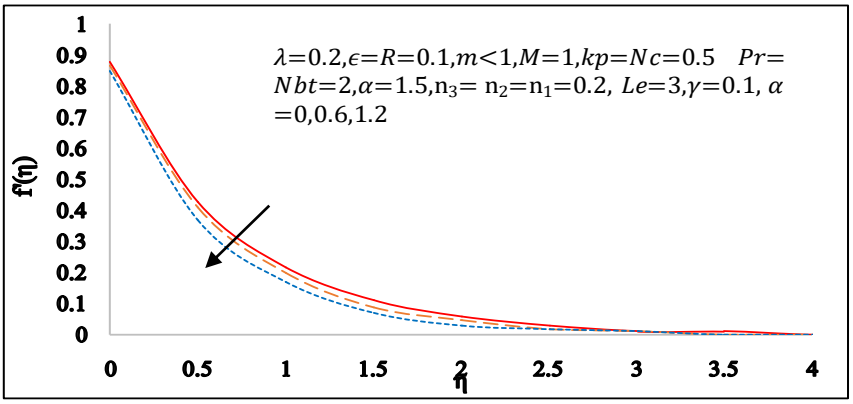

Figure 9. Impact of α on f'

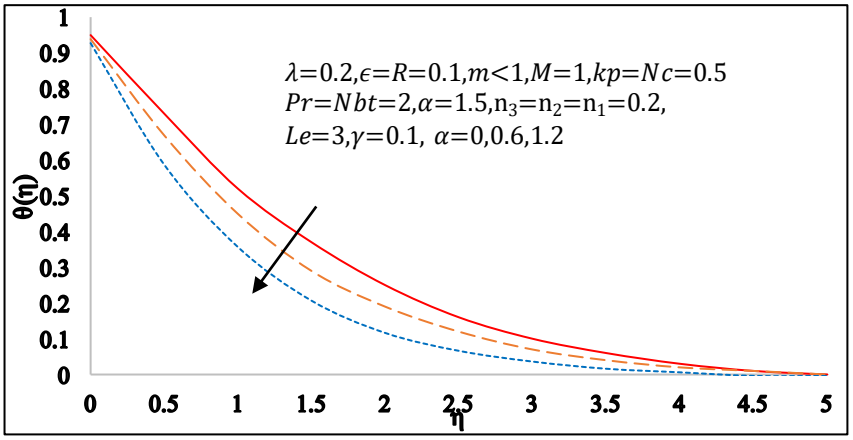

Figure 10. Impact of α on θ

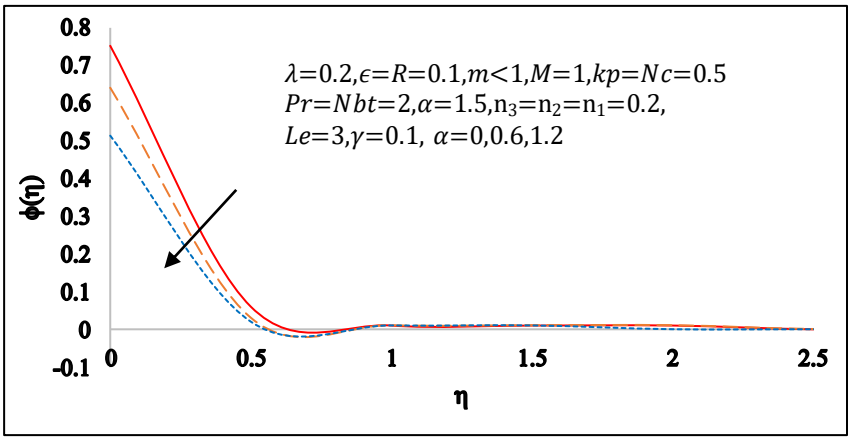

Figure 11. Impact of α on ϕ

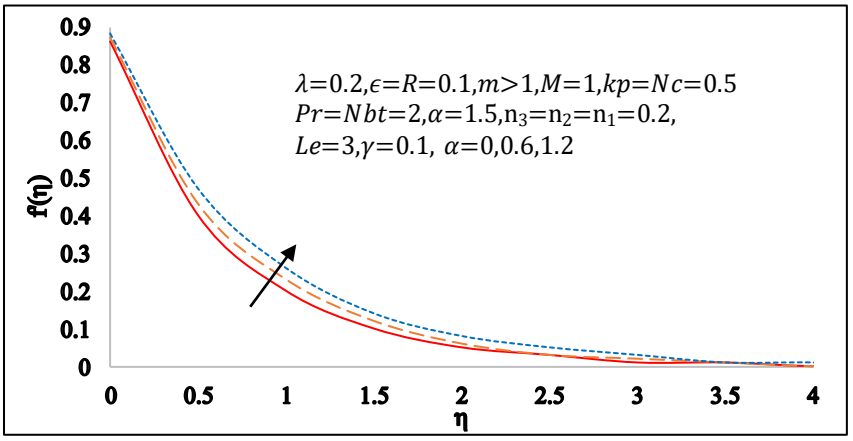

Figure 12. Impact of α on f'

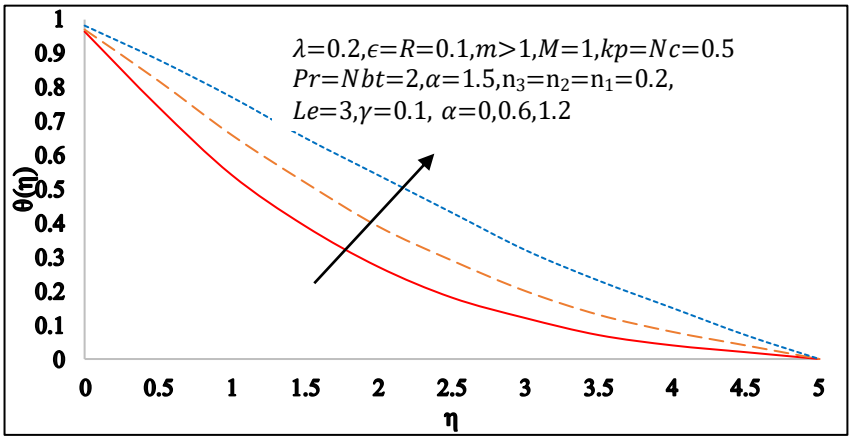

Figure 13. Impact of α on θ

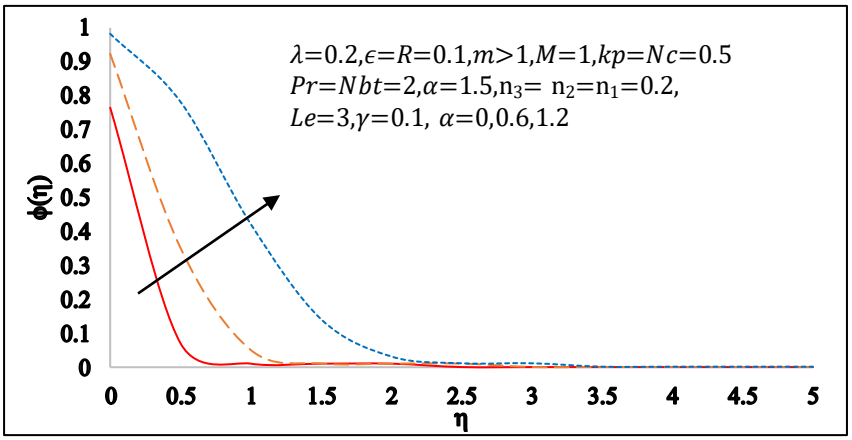

Figure 14. Impact of α on ϕ

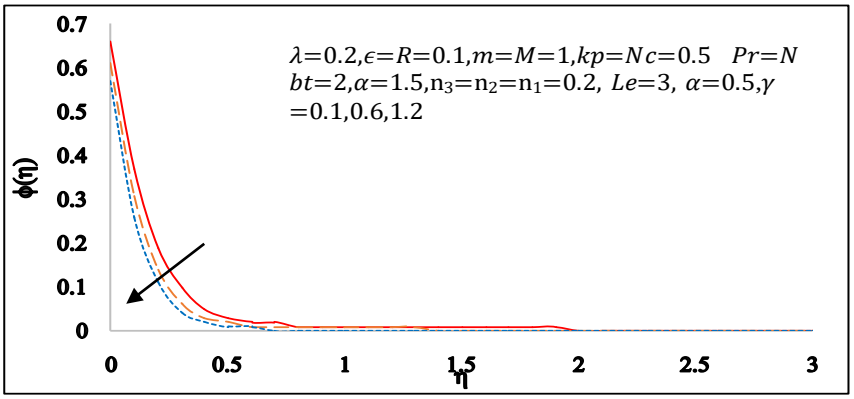

Figure 15. Impact of γ on ϕ

5. CONCLUSION

On the basis of the analysis of solution, the following results are obtained.

- The velocity profile has been decreased for an increase of n_1, n_2, n_3, α with $m<1$ and slightly increased for increasing of m, increased for more than one of m.
- The variation of temperature has been decreased for an increase of its slip parameter, wall thickness parameter for less than one of m, but increased for the raising values of m.
- The profile of nanoparticle volume fraction has been decreased by increasing value of γ.
- The concentration profile has been reduced for the raising the value of γ.

NOMENCLATURE

$(\bar{u}, \bar{v})$ Velocity components along the X,Y axes

ρ Density of the nanofluid

σ Electrical conductivity

Ƙ Temperature dependent thermal conductivity

Tw Wall temperature of fluid,

T_∞ Ambient temperature

$(\rho c)_p$ Effective heat capacity of the nanoparticle

$(\rho c)_f$ Effective heat capacity of the nanofluid

D_B Brownian diffusion Coefficient

D_T Coefficient of thermophoresis diffusion

B_0 Induced magnetic field

q_r Roseland approximation

λ Non- Newtonian Williamson Parameter

M Magnetic parameter

Kp Permeability Parameter

Pr Prandtl number

Le Lewis Number

CONFLICT OF INTERESTS

The authors declare that there is no conflict of interests.

REFERENCES

[1] S.U.S. Choi, J. Eastman, Enhancing Thermal Conductivity of Fluids with Nanoparticles. Lemont, IL: Argonne National Lab; 1995:99–105.

[2] J. Buongiorno, Convective transport in nanofluids. ASME J. Heat Transf. 128 (2006), 240–250.

[3] W. Daungthongsuk, S. Wongwises, A critical review of convective heat transfer of nanofluids, Renew. Sustain. Energy Rev. 11 (2007), 797–817.

[4] X.Q. Wang, A.S. Mujumdar, A review on nanofluids part I: theoretical and numerical investigations, Brazil J. Chem. Eng. 25 (2008), 613-630.

[5] X.Q. Wang, A.S. Mujumdar, review on nanofluids part II: experiments and applications, Brazil. J. Chem. Eng. 25 (2008), 631-648.

[6] S. Kakac, A. Pramuanjaroenkij, Review of convective heat transfer enhancement with nanofluids, Int. J. Heat. Mass. Transf. 52 (2009), 3187-3196.

[7] A.V. Kuznetsov, D.A. Nield, Natural convective boundary- layer flow of a nanofluid past a vertical plate, Int. J. Therm. Sci. 49 (2010), 243-247.

[8] N. Bachok, A. Ishak, I. Pop, Boundary-layer flow of nanofluids over a moving surface in a flowing fluid, Int. J. Therm. Sci. 49 (2010), 1663-1668.

[9] W.A. Khan, I. Pop, Boundary-layer flow of a nanofluid past a stretching sheet Int. J. Heat. Mass. Transf. 53 (2010), 2477-2483.

[10] P.Rana, R. Bhargava, Flow and heat transfer of a nanofluid over a nonlinearly stretching sheet: a numerical study, Commun. Nonlinear Sci. Numer. Simul. 17 (2012), 212-226.

[11] G.K. Ramesh, B.J. Gireesha, B.C. Kumara, R.S. Gorla, MHD stagnation point flow of nanofluid towards a stretching surface with variable thickness and thermal radiation, J. Nanofluids. 4 (2015), 247-253.

[12] T.R. Mahapatra, A.S. Gupta, Magneto hydrodynamic stagnation-point flow towards a stretching sheet, Acta Mech. 152 (2001), 191-196.

[13] S. Mahmud, M.M. Rashidi, Navid Freidoonimehr, Unsteady MHD free convective flow past a permeable stretching vertical surface in a nano-fluid, Int. J. Therm. Sci. 87 (2015), 136-145.

[14] M.M. Rashidi, E. Momoniat, B. Rostami, Analytic approximate solutions for MHD boundary-layer viscoelastic fluid flow over continuously moving stretching surface by homotopy analysis method with two auxiliary parameters, J. Appl. Math. 2012 (2012), Article 780415.

[15] R.V. Williamson, The flow of pseudo plastic materials, Ind. Eng. Chem. 21 (1929), 1108-1111.

[16] S. Nadem, S.T. Hussain, Flow and heat transfer analysis of Williamson nanofluid, Appl. Nanosci. 4 (2014), 1005-1012.

[17] S. Nadeem, S.T. Hussain, Analysis of MHD Williamson nano fluid flow over a heated surface, J. Appl. Fluid Mech. 9 (2016), 729-739.

[18] M.M. Khader, A.M. Megahed, Numerical solution for boundary layer flow due to a nonlinearly stretching sheet with variable thickness and slip velocity, Eur. Phys. J. Plus. 128 (2013), 100.

[19] S. Reddy C, K. Naikoti, M.M. Rashidi, MHD flow and heat transfer characteristics of Williamson nanofluid over a stretching sheet with variable thickness and variable thermal conductivity, Trans. A. Razmadze Math. Inst. 171 (2017), 195–211.

[20] S.M. Razi, S.K. Soid, A.S. Abd Aziz, N. Adli, Z.M. Ali, Williamson nanofluid flow over a stretching sheet with varied wall thickness and slip effects, J. Phys.: Conf. Ser. 1366 (2019), 012007.